A. Mimani, C. J. Doolan, and P. R. Medwell

**Multiple line arrays for the characterization of aeroacoustic sources using a time-reversal method**

Journal of the Acoustical Society of America, 2013; 134(4):327-333

# Multiple line arrays for the characterization of aeroacoustic sources using a time-reversal method

**A. Mimani,[a] C. J. Doolan, and P. R. Medwell**
*School of Mechanical Engineering, The University of Adelaide, South Australia 5005, Australia*
*akhilesh.mimani@adelaide.edu.au, con.doolan@adelaide.edu.au, paul.medwell@adelaide.edu.au*

**Abstract:** This letter investigates the use of multiple line arrays (LAs) in a Time-Reversal Mirror for localizing and characterizing multipole aeroacoustic sources in a uniform subsonic mean flow using a numerical Time-Reversal (TR) method. Regardless of the original source characteristics, accuracy of predicting the source location can be significantly improved using at least two LAs. Furthermore, it is impossible to determine the source characteristics using a single LA, rather a minimum of two are required to establish either the monopole or dipole source nature, while four LAs (fully surrounding the source) are required for characterizing a lateral quadrupole source.


**PACS numbers:** 43.60.Tj, 43.60.Jn, 43.60.Fg, 43.20.Rz [CG]
**Date Received:** June 26, 2013 **Date Accepted:** August 11, 2013

## 1. Introduction

The use of Time-Reversal (TR) for aeroacoustics promises to provide greater insight into the noise-generating physics.[1,2] There are many uncertainties in the use of TR in this application, one of which concerns the number and type of microphone line arrays (LAs) that can be used. TR simulations performed using a limited angular aperture line array (LA) in a Time-Reversal Mirror (TRM) that only partially encloses a source, captures only a small fraction of the acoustic pressure radiated. This limits the ability of TR to identify the location and nature of the source region.[3] However, a microphone LA configuration in a TRM completely enclosing the source intercepts the acoustic wave propagating in all directions.[3,4] Naturally, this LA configuration yields the most accurate prediction of the source location, and the shape and strength may also be recovered exactly.[2,4] However, setting up of such a LA configuration may be difficult in an aeroacoustics experiment conducted in an anechoic wind tunnel[1] due to the number of microphones required and because the microphone locations may be restricted to regions outside the flow field. Padois *et al.*[1] use acoustic pressure time-history measured over one LA of microphones in a TRM (located above a wind tunnel test area and outside the flow) to localize time-harmonic monopole and dipole sources in wind tunnel flows using numerical TR simulations. The axis of the dipole source (modeled by two speakers out-of-phase) was parallel to the flow. However, the practically relevant cases of a dipole with its axis perpendicular to the flow (such as a cylinder in uniform mean flow[5]) or a quadrupole (such as free turbulence[6]) were not considered.

The main limitation in the work of Padois *et al.*[1] is the use of one LA in a TRM which cannot record sufficient acoustic pressure time-history data required during TR simulations for resolving a dipole source with an axis perpendicular to flow. The out-of-phase radiation pattern about the mean flow direction of this dipole source implies that one LA can capture only half the phase information, and therefore, would incorrectly predict a monopole source. By means of TR simulations based on the Pseudo-Characteristic Formulation[7] (PCF), Deneuve *et al.*[2] show that the shape and

[a]Author to whom correspondence should be addressed.

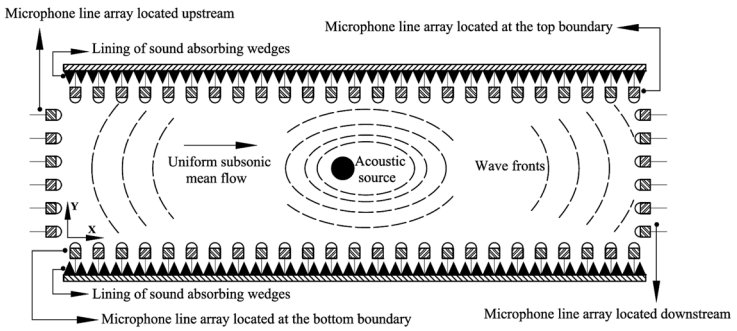


Fig. 1. A schematic of an anechoic wind tunnel with microphone LAs in a TRM located at the boundaries for recording the acoustic pressure field radiated by an aeroacoustic source (direction of mean flow indicated).

strength of a Gaussian pulse (in 2-D rectangular domain) obtained using one LA, (i.e., the boundary data) are significantly different from the initial pulse hinting at the need for multiple LAs in a TRM for accurate characterization of aeroacoustic sources. Harker and Anderson[8] obtained an optimized TRM comprising of a LA of microphones located on a circular arc, either fully or partially surrounding a source in terms of angular spacing and aperture for localizing a harmonic monopole source.

The use of multiple LAs in a TRM has the potential to improve the performance of the TR method for aeroacoustic applications, yet it has not been studied in previous work.[1] Therefore, this Letter presents new, multiple LA simulations that quantifies the improvements in both accuracy and source characterization for monopole, dipole, and quadrupole sources in subsonic cross-flow. The practical importance of the work is seen in obtaining guidelines for designing an aeroacoustic experiment involving acoustic pressure measurements over microphone LAs in a TRM located at the boundaries of an anechoic wind tunnel shown by a schematic in Fig. 1.

## 2. Summarized implementation of numerical method

An algorithm is outlined for numerical implementation of the forward and TR method on a 2-D rectangular computational domain $|y| \leq L_y$, $|x| \leq L_x$, where $L_x = L_y = 0.5$ m. The forward simulations were performed by numerically solving the inhomogeneous 2-D Linearized Euler Equations (LEE) with a subsonic uniform mean flow of Mach number $M_0 = 0.3$ along the positive $x$ direction and zero mean flow along the $y$ direction using the PCF.[7] The spatial derivatives of acoustic pressure and acoustic particle velocities in the fluxes propagating along opposite directions are computed using an overall upwind biased Finite-Difference (FD) scheme formulated using the fourth order, 7-point optimized upwind biased FD scheme[9] at the interior nodes and 7-point optimized backward FD scheme[10] at the boundary nodes. The inhomogeneous source term that simulates a time-harmonic aeroacoustic source (such as idealized monopole, dipole and quadrupole) of frequency $f = 3000$ Hz is adopted from Bailly and Juve.[11] The center of the domain (set to be the origin in all presented results) is taken as the known source location. The monopole source strength is taken as $1 \times 10^{-3}$ m$^2$ s$^{-1}$, the dipole and quadrupole sources are simulated by a fluctuating force of amplitude 1 N m$^{-2}$ and Lighthill's stress tensor of amplitude 1 N m$^{-2}$, respectively. The domain is discretized into equally spaced nodes of mesh sizes $\Delta x = \Delta y = 0.01$ m along the $x$ and $y$ directions, respectively, while $c_0 = 343.14$ m s$^{-1}$ is the sound speed. The ambient density $\rho_0$ is taken as 1.21 kg m$^{-3}$. The third order Total Variation Diminishing (TVD) Runge–Kutta scheme[12] is used for time-integration during the forward and TR simulations. The *CFL* number equal to 0.05 is considered during the forward simulations to ensure stability and accuracy. The first-order Clayton-Engquist-Majda (CEM) anechoic boundary conditions[13] (BCs) and the corner anechoic BCs[14] at the four corner nodes

were implemented. The forward simulations were implemented for a large interval $t=[0,\ T_{\max}=N_{\max}\,\Delta t]$ during which the zero-initial conditions were replaced with several periods of steady-state response, while the acoustic pressure $\tilde{p}(x,y,\ t)$ time-history was stored at nodes (virtual microphones of spacing equal to the mesh size) of all four boundaries. (Here, $\Delta t = 1.1209\times10^{-6}$ s is the time-step and $N_{\max}=12\,000$.)

The TR simulation was implemented by setting the source term to zero, reversing (a) the mean flow direction[1] and (b) the forward time ($t \rightarrow T_{\max}-\tilde{t}$) and enforcing the time-reversed $\tilde{p}\ (x,\ y,\ \tilde{t})$ history[1,2] at nodes in a TRM configuration corresponding to either (1) one LA located at the top ($y=L_y$) boundary, (2) two LAs located at the top and bottom ($y=-L_y$) boundaries, (3) three LAs located at the top, bottom and right ($x=L_x$) boundaries, and (4) all the four boundaries ($y=\pm L_y,\ x=\pm L_x$), i.e., four LAs fully surrounding the source over the interval $\tilde{t}=[0,\ T_{\max}]$, where $\tilde{t}$ represents reversed time. First-order CEM anechoic BCs[13] and corner BCs[14] were implemented to eliminate reflections. However, while using multiple LAs, the flux emanating from one of the LAs passes through the source region (due to absence of an acoustic sink[15]), propagates further, impinges and interferes with the incoming flux that emanates from the LA located at the opposite boundary. For diminishing the deteriorating effect of this interference, the incoming flux normal to the LAs is damped (across the five nodes adjacent to the LA boundary) while leaving the outgoing waves unaffected. The fluxes propagating toward anechoic boundaries are however, left unchanged. This unidirectional damping technique based on damping only the fluxes which propagate toward the LA without affecting the fluxes that propagate away from the LA into the domain, is termed as the Time-Reversal-Sponge-Layer (TRSL) and is used during the TR simulations involving multiple LAs in a TRM in a rectangular domain.

### 3. Simulation results and discussions

The location(s) of time-harmonic aeroacoustic source(s) in the computational domain is (are) obtained by determining the region(s) of maximum magnitude in the Root-Mean-Square (RMS) time-reversed acoustic pressure field. These regions of maximum RMS magnitude are called focal spots. The RMS of the time-reversed acoustic pressure field [denoted as $\tilde{p}^{\mathrm{TR}}_{\mathrm{RMS}}\ (x,\ y)$] is calculated over the time-interval corresponding to when a steady state TR acoustic field is established over the entire computational domain.[1] Figure 2 depicts the $\tilde{p}^{\mathrm{TR}}_{\mathrm{RMS}}(x,\ y)$ field computed using the time-reversed $\tilde{p}(x,\ y,\ \tilde{t})$ history of the idealized monopole source (the same test case as Ref. 1) from (a) one LA, (b) two LAs, (c) three LAs, and (d) four LAs fully surrounding the source. The colorbar indicates the magnitude in dB with reference to 20 $\mu$Pa. The known and predicted source locations are indicated by a circle **O** and a cross **X,** respectively, whereas the "reversed" direction of mean flow is indicated by an arrow. The thick white lines signify a LA at the particular boundary. The same symbol and unit conventions are also followed for the remaining results. In Fig. 2(a), the monopole source location is predicted from the maximum of the elongated focal spot[1] at $x=0$, $y=0.04$ m. The discrepancy between the predicted and known source location is $0.35\lambda$, where $\lambda$ is the wavelength. The $\tilde{p}^{\mathrm{TR}}_{\mathrm{RMS}}\ (x,\ y)$ field in Figs. 2(b)–2(d) exhibit a central focal spot of enhanced magnitude and diminished width, and the predicted monopole source location is co-incident with the known location. This demonstrates an increase in source resolution using multiple LAs and a significant improvement in the accuracy of prediction of monopole source location using at least two LAs in a TRM.

The case of a dipole source with its axis perpendicular to the flow direction is presented in Fig. 3. To enhance the understanding, the TR simulations using (a) one LA in a TRM located at $y=L_y$ boundary simulated in Mm. 1 and (b) two LAs in a TRM located at $y=\pm L_y$ boundaries simulated in Mm. 2 may also be referred. (The colorbar in each of the multimedia files indicates the acoustic pressure in Pa.)

Mm.1. TR simulation using one LA located at $y=L_y$. This is a "avi" file (9.95 Mb).

Mm.2. TR simulation using two LAs located at $y=\pm L_y$. This is a "avi" file (9.76 Mb).

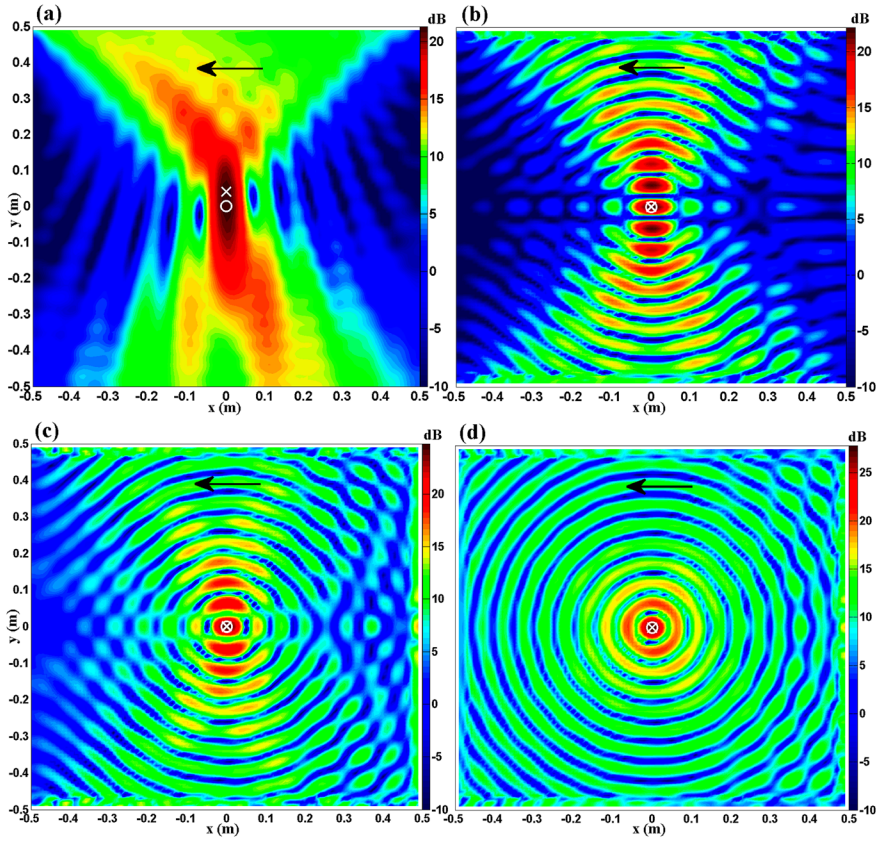


Fig. 2. (Color online) The $\tilde{p}^{\mathrm{TR}}_{\mathrm{RMS}}(x, y)$ field due to an idealized monopole source obtained using a TRM comprising of (a) single LA at $y = L_y$ boundary, (b) two LAs at $y = \pm L_y$ boundaries, (c) three LAs at $y = \pm L_y$, $x = L_x$ boundaries and (d) four LAs fully surrounding the source.

The $\tilde{p}^{\mathrm{TR}}_{\mathrm{RMS}}(x, y)$ field in Fig. 3(a) obtained using one LA shows an elongated focal spot similar to that obtained in the monopole case [Fig. 2(a)]. This demonstrates that one LA in a TRM located parallel to the mean flow is inadequate to resolve a dipole source with its axis perpendicular to the flow direction. A discrepancy of $0.35\lambda$ is also observed in the predicted dipole source location in Fig. 3(a). The $\tilde{p}^{\mathrm{TR}}_{\mathrm{RMS}}(x, y)$ field in Fig. 3(b) obtained using two LAs, however, indicates the presence of two focal spots (in proximity) of equal magnitude and offset on the $y$ axis by an equal distance. The dipole source location predicted from the geometrical center of maximum of the two focal spots (located at $x_{f_1} = x_{f_2} = 0$, $y_{f_1,f_2} = \pm 0.03$ m) in Fig. 3(b) is $x = y = 0$ which is co-incident with the known source position. This illustrates that two LAs in a TRM located parallel to the mean flow and either side of the source are necessary to accurately localize and resolve a dipole source when its axis is perpendicular to the mean flow. (The co-ordinates $(x_{f_i}, y_{f_i})$ correspond to the maximum point of the $i$th focal spot and the same convention is followed, henceforth.) Figure 3(c) obtained using four LAs fully surrounding the source exhibits a further enhanced resolution of the two focal spots, while the predicted and known locations are co-incident. It may be concluded the accuracy of prediction of dipole source location not only improves significantly with the use of two LAs, rather given the apparent similarity between Figs. 2(a) and 3(a), two LAs are required to resolve the difference between a monopole and higher-order source. In order to confirm the dipole source nature, it has also been shown that the time-reversed acoustic pressure histories at the maxima of each of the

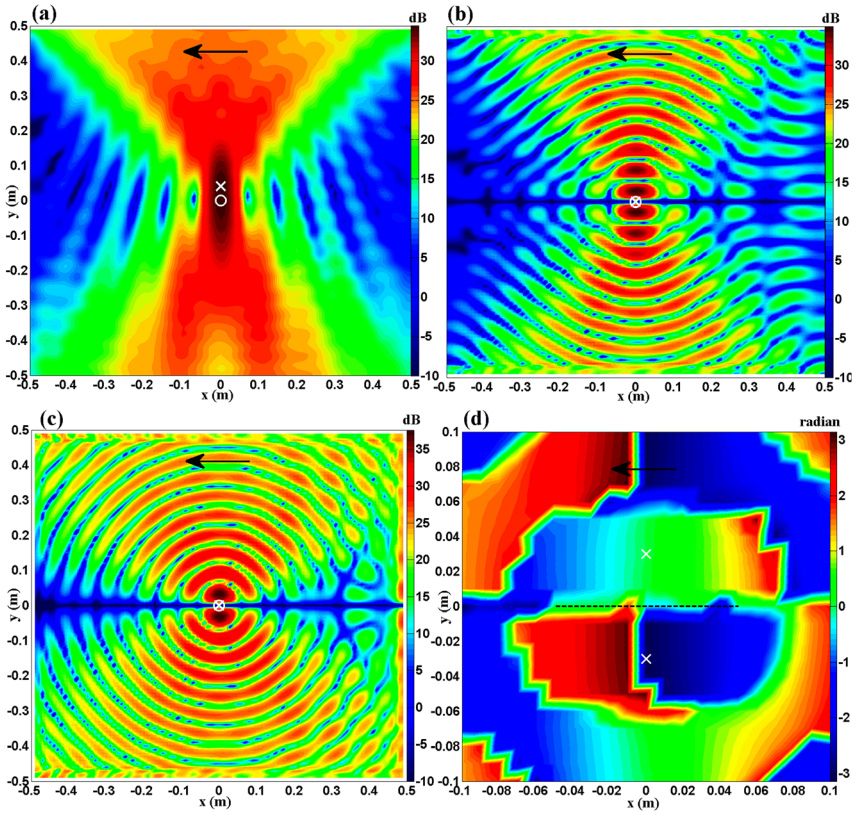


Fig. 3. (Color online) The $\tilde{p}^{\mathrm{TR}}_{\mathrm{RMS}}(x, y)$ field due to an idealized dipole source with its axis perpendicular to the mean flow obtained using a TRM comprising of (a) single LA at $y = L_y$ boundary, (b) two LAs at $y = \pm L_y$ boundaries, and (c) four LAs fully surrounding the source. (d) The relative phase variation $\phi(x, y)$ (in radian) of local $\tilde{p}(x, y, \tilde{t})$ over the region enclosing the two focal spots obtained in (b). (The cross X represents the two focal points.)

two focal spots in Figs. 3(b) and 3(c) are $\pi$ radian out of phase.[1,16] This result may also be confirmed by inspecting the TR simulations in Mm. 2 Figure 3(d) shows the variation of relative phase $\phi(x, y)$ in the acoustic pressure histories with respect to the focal point $(x_{f_1}, y_{f_1})$ over the small region enclosing the two focal points in Fig. 3(b), wherein $\phi$ of the focal point $(x_{f_2}, y_{f_2})$ is $\pi$, thereby establishing the dipole nature.[16]

Figures 4(a)–4(c) shows the TR simulation results for a lateral quadrupole source with its axes perpendicular to the $x$ and $y$ directions. Figure 4(a) (one LA) shows an elongated focal spot, therefore incorrectly predicting the existence of a source at $x = 0.02$ m, $y = 0.11$ m which deviates significantly from the known quadrupole source location (placed at the origin) by $0.98\lambda$. In Fig. 4(b), with the use of two LAs in a TRM, the quadrupole source location is predicted at $x = 0.01$ m, $y = 0$ (an error of $0.08\lambda$), indicating a substantial improvement in accuracy. Nonetheless, two LAs cannot resolve the quadrupole source characteristics as may be inferred from Fig. 4(b). The $\tilde{p}^{\mathrm{TR}}_{\mathrm{RMS}}(x, y)$ field obtained using three LAs (not shown in this Letter) can resolve a lateral quadrupole, however, as shown in Fig. 4(c), the use of four LAs fully surrounding the source yields the most accurate focal spot resolution. In Fig. 4(c), four distinct focal spots (located in proximity) are observed; suggesting that four LAs completely enclosing the source is ideally suited to resolve a quadrupole source. The maximum of the four focal spots are located at $(x_{f_1,f_2}, y_{f_1,f_2}) = (\mp 0.05\,\mathrm{m}, 0)$ and $(x_{f_3,f_4}, y_{f_3,f_4}) = (0, \pm 0.05\,\mathrm{m})$ and the separation distance ($0.87\ \lambda$) between the maximum of the two focal spots located on opposite corners of the square indicates a higher-order source. The quadrupole source

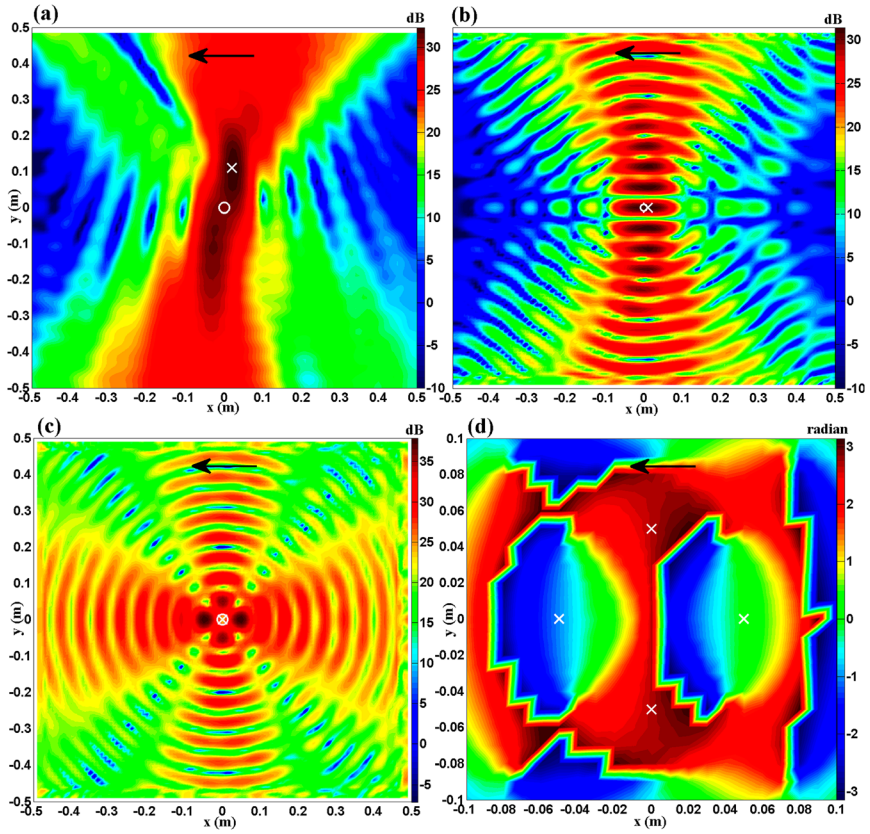


Fig. 4. (Color online) The $\tilde{p}^{TR}_{RMS}(x, y)$ field due to an idealized lateral quadrupole source with its axes perpendicular to the $x$ and $y$ directions obtained using a TRM comprising of (a) single LA at $y = L_y$ boundary, (b) two LAs at $y = \pm L_y$ boundaries and (c) four LAs fully surrounding the source. (d) The relative phase variation $\phi(x, y)$ (in radian) of local $\tilde{p}(x, y, \tilde{t})$ over the region enclosing the four focal spots obtained in (c). (The cross X represents the four focal points.)

location is taken as the geometrical center of the four focal spots, hence $x = y = 0$ indicating the co-incidence of predicted and known locations. The quadrupole source nature is confirmed by quantifying $\phi$ between the local time-reversed acoustic pressure histories at the maximum of the four focal spots in Fig. 4(c). The $\phi$ between the $\tilde{p}(x, y, \tilde{t})$ time-histories at (1) $(x_{f_1}, y_{f_1})$ and $(x_{f_2}, y_{f_2})$ is equal to 0.32 $\pi$ radian, indicating a significant deviation from in-phase radiation of the maxima points $f_1$ and $f_2$ due to the convective effect of mean flow,[1] (2) $(x_{f_3}, y_{f_3})$ and $(x_{f_4}, y_{f_4})$ is zero indicating that the maxima points $f_3$ and $f_4$ are exactly in-phase, (3) $(x_{f_3}, y_{f_3})$ and $(x_{f_1}, y_{f_1})$ is $0.83\pi$ radian, and (4) $(x_{f_3}, y_{f_3})$ and $(x_{f_2}, y_{f_2})$ is $0.84\pi$ radian, signifying small deviation from out-of-phase radiation between the two adjacent pairs of maxima points in (3) and (4) due to the convective effect of mean flow.[1] Nonetheless, the $\phi$ values indicate that four focal points in Fig. 4(c) have alternating phase, hence representing a lateral quadrupole source. These observations may be confirmed from Fig. 4(d) by examining the variation of $\phi(x, y)$ with respect to the focal point $(x_{f_2}, y_{f_2})$ over a small region enclosing the four focal spots obtained in Fig. 4(c).

## 4. Conclusions

The use of a single LA in a TRM yields typically an error (approximately the order of $\lambda$) in the predicted source location; however, it does not properly characterize the nature of the source. Regardless of the source characteristics, the use of at least two LAs in a

TRM not only reduces the error in predicted source location but also allows insight into the nature of source. Using two LAs, a dipole source is revealed if the $\tilde{p}^{TR}_{RMS}(x, y)$ field exhibits two focal spots of nearly equal magnitude located in proximity, whereas a monopole is indicated if the $\tilde{p}^{TR}_{RMS}(x, y)$ field exhibits a central focal spot flanked by focal spots of significantly lesser magnitudes. An elongated central focal spot flanked by similar focal spots of nearly the same magnitude suggests a higher-order source and requires more than two LAs (increase in aperture of the TRM) for proper resolution. The results presented here can be used for determining the minimum number of microphone LAs in a TRM that are needed to resolve higher-order aeroacoustic sources experimentally in an anechoic wind tunnel. For instance, the case of a uniform cylinder located in a mean flow (with axis perpendicular to the flow) in a wind tunnel resembles a dipole source with its axis perpendicular to flow,[5] therefore, two LAs in a TRM at the top and bottom boundaries are required for localizing and characterizing the source. Furthermore, the requirement of four LAs in a TRM completely surrounding the source for the proper resolution of a lateral quadrupole implies that microphone LAs may need to be placed within the flow, therefore, characterizing a quadrupole experimentally using TR method is challenging and requires further investigation.

## Acknowledgments

The authors are grateful to Professor Vincent Valeau for helpful discussions and suggestions. This work was supported by the Australian Research Council (ARC) under grant DP 120102134 "Resolving the mechanics of turbulent noise production."

## References and links

[1]T. Padois, C. Prax, V. Valeau, and D. Marx, "Experimental localization of an acoustic source in a wind-tunnel flow by using a numerical time-reversal technique," J. Acoust. Soc. Amer. **132**, 2397–2407 (2012).
[2]A. Deneuve, P. Druault, R. Marchiano, and P. Sagaut, "A coupled time-reversal/complex differentiation method for aeroacoustic sensitivity analysis: Towards a source detection procedure," J. Fluid Mech. **642**, 181–212 (2010).
[3]M. Fink and C. Prada, "Acoustical time-reversal mirrors," Inverse Probl. **17**, R1–R38 (2001).
[4]M. Fink, D. Cassereau, A. Derode, C. Prada, P. Roux, M. Tanter, J. L. Thomas, and F. Wu, "Time-reversed acoustics," Rep. Prog. Phys. **63**, 1933–1995 (2000).
[5]W. K. Blake, *Mechanics of Flow-Induced Sound and Vibration* (Academic Press, New York, 1986), Vol. 1, pp. 64, 65, 219–283.
[6]M. J. Lighthill, "On sound generated aerodynamically—I. General Theory," Proc. R. Soc. Lond. Ser. A **211**, 564–587 (1952).
[7]J. Sesterhenn, "A characteristic-type formulation of the Navier-Stokes equations for high order upwind schemes," Comput. Fluids. **30**, 37–67 (2001).
[8]B. M. Harker and B. E. Anderson, "Optimization of the array mirror for time reversal techniques used in half-space environment," J. Acoust. Soc. Amer. **133**, EL351–EL357 (2013).
[9]M. Zhuang and R. F. Chen, "Applications of high-order optimized upwind schemes for computational aeroacoustics," AIAA J. **40**, 443–449 (2002).
[10]C. K. W. Tam, "Computational aeroacoustics: Issues and methods," AIAA J. **33**, 1788–1796 (1995).
[11]C. Bailly and D. Juve, "Numerical solution of acoustic wave propagation problems using linearized Euler equations," AIAA J. **38**, 22–29 (2000).
[12]S. Gottlieb and C.-W. Shu, "Total variation diminishing Runge-Kutta schemes," Math. Comput. **67**, 73–85 (1998).
[13]R. Clayton and B. Engquist, "Absorbing boundary conditions for acoustic and elastic wave equations," Bull. Seism. Soc. Am. **67**, 1527–1540 (1977).
[14]B. Engquist and A. Majda, "Radiation boundary conditions for acoustic and elastic wave calculations," Commun. Pur. Appl. Math. **32**, 313–357 (1979).
[15]E. Bavu and A. Berry, "High-resolution imaging of sound sources in free field using a numerical time-reversal sink," Acta. Acust. Acust. **95**, 595–606 (2009).
[16]A. Mimani, C. J. Doolan, and P. R. Medwell, "Localisation of a stationary time-harmonic dipole sound source in flows using time-reversal simulation," in *Proceedings of Acoustics 2013*, Victor Harbor, Australia (November 17–20, 2013), p. 13.